

Transition voltage spectroscopy: a challenge for vacuum tunneling models at nanoscale

Ioan Bâldea* and Horst Köppel

Theoretische Chemie, Universität Heidelberg, Im Neuenheimer Feld 229, D-69120 Heidelberg, Germany

Several recent studies on the transition voltage (V_t) of molecular and vacuum nano-junctions are based on calculations of the tunneling current through an energy barrier within the so-called Simmons model, which is an approximate WKB-type approach developed for thin insulating films with infinite transverse extension. In this paper devoted to vacuum nano-junctions, we compare the Simmons results for V_t with those obtained from the exact Schrödinger equation by exactly including the classical (non-retarded) charge image effects. The comparison reveals that the Simmons estimates for V_t are completely unacceptable for nanogap sizes (d) at which image effects are important. The Simmons treatment drastically overestimates these effects, because it misses the famous $1/2$ factor related to the fact that the image interaction energy is a self energy. The maximum of the Simmons curve V_t vs. d turns out to be merely an artefact of an inappropriate approximation. Unlike the Simmons approach, the “exact” WKB method yields results, which qualitatively agree with the exact ones; quantitative differences are important, demonstrating that the transmission prefactor has a significant impact on V_t . Further, we show that a difference between the work functions of (say,) the left and right electrodes, which gives rise to a Volta intrinsic field, may be important for the ubiquitous asymmetry of the measured I - V -characteristics [$I(V) \neq -I(-V)$] in general, and for the different V_t -values at positive and negative biases reported in vacuum nano-junctions in particular. The weak dependence $V_t = V_t(d)$ found experimentally in vacuum nano-junctions contrasts to the pronounced dependence obtained by including the exact electrostatic image contribution into the exact Schrödinger equation. This demonstrates that not only the molecular transport, but also the transport through a vacuum nano-gap represents a nontrivial problem, which requires further refinements, e. g, a realistic description of contacts’ geometry, retardation effects due to the finite tunneling time, local phonons, surface plasmons or electron image states.

PACS numbers: 73.63.Rt, 85.35.Gv 85.65.+h,

I. INTRODUCTION

In the continuous efforts for miniaturization, using single molecules as active components for future nanoelectronic devices appears at present as the only conceivable alternative, which escapes the fundamental limitations of complementary metal-oxide semiconductor (CMOS) technologies. In molecular devices, electron transfer between the source (S) and drain (D) electrodes across the nanogap (width d) can occur via through-bond and through-space processes. In these processes, electrons have to tunnel through an energy barrier given by the energy offset $\varepsilon_B = \min(\varepsilon_F - \varepsilon_{HOMO}, \varepsilon_{LUMO} - \varepsilon_F)$ of the closest molecular orbital (HOMO or LUMO) from electrodes’ Fermi level (ε_F) and the metallic work function W , respectively. Similar to electron transfer in numerous chemical reactions, through-bond and through-space processes can compete, because (i) in usual off-resonance situations, the Fermi level lies close to middle of the HOMO-LUMO gap (charge neutrality), and ε_B amounts several electronvolts, i. e., only slightly smaller than W and (ii) charge image effects, which narrow, round, and lower the barrier,^{1,2} are more pronounced in vacuum than in molecules due to the different dielectric constants [$\kappa_r \equiv 1$ versus $\kappa_r \approx 2 - 3$, respectively, cf. Eq. (9) below]. Concerns that the measured currents are not (or not only) due to the active molecules have plagued the field of molecular electronics since its inception.³ For a proper interpretation of transport experiments, through-bond and through-space mechanisms should be each correctly un-

derstood.

Transition voltage spectroscopy (TVS) has been proposed recently as an appealing tool to deduce ε_B , a key parameter for molecular junctions.⁴⁻⁷ TVS relies upon simple intuitive considerations inspired by the barrier picture. The initial TVS conjecture was that the minimum $V = V_t$ of the Fowler-Nordheim (FN) curves [$\log(I/V^2)$ versus $1/V$, obtained by recasting the source-drain I - V -characteristics] suffices to determine the molecular energy offset: $eV_t = \varepsilon_B$. This minimum was ascribed to the point where the shape of the energy barrier tilted by the applied voltage V ($\varepsilon_B \rightarrow \varepsilon_B - eVx/d$, where x specifies the position) changes from trapezoidal to triangular. Calculations of the tunneling current within the Simmons’ model⁸ challenged the validity of the barrier description for molecular junctions,⁹ claiming that it yields a dependence of V_t on ε_B and d disagreeing with experiments.^{4-7,10} Based on them, it was suggested that the dependence $V_t = V_t(d)$ ⁹ or the magnitude of V_t ¹¹ can be used to discriminate between through-bond and vacuum tunneling. Some aspects of the TVS in molecular junctions^{9,12-14} and gated single-molecule transistors¹⁵ received theoretical consideration.

Letting alone the fact that the calculations of Ref. 9 used the Simmons’ approximation⁸ (an issue to be addressed in detail in the present paper), it is worth emphasizing that those calculations disregarded an important fact. Namely, that in order to phenomenologically model the tunneling through a molecule, it is too simplistic that, irrespective of the molecule under consider-

ation, electrons within the barrier (“molecule”) be generally characterized by the free electron mass m . Several studies drew attention on the fact that this is an illegitimate assumption,^{16,17} and one rather needs to employ an effective mass m^* , which is molecule specific [with the present notations $m^* = m^*(d, \varepsilon_B)$]. For the above reasons, the utilization of the barrier picture for molecular transport is only possible if the phenomenological parameters ε_B and m^* are determined by fitting experimental data or from companion ab initio calculations.

While modeling the active molecule as an energy barrier may be too simplistic, and describing the electrons that tunnel in molecules (unless they possess delocalized π electrons) within the effective mass approximation questionable, the barrier picture appears as the most natural framework for studying the transport in vacuum nanojunctions. Still, it is only recently that a theoretical study becomes attractive, because, in contrast to the immense number of studies on molecular junctions (a very incomplete list includes Refs. 4–7,10,18–23 and citations therein) experiments on electron tunneling through vacuum in nanojunctions have been carried out only very recently.¹¹

Among very numerous approaches to the electron transport by tunneling relying upon the barrier picture,^{1,2,24–32} an approach due to Simmons⁸ became increasingly popular for the interpretation of important experimental findings in molecular-/nanojunctions.^{4–7,10,16,17,19,33} This popularity among experimentalists should certainly be related to the fact that, unlike in other (more accurate, see, e. g., Ref. 31) treatments, Simmons gave approximate but simple analytic formulas, which can be easily used for fitting experimental data. While primarily discussing and formulating the barrier approach to nanojunctions in general, we will also to draw attention on the fact that Simmons’ formulas, aiming to describe thin insulating films, are not appropriate for molecular/nano-transport. An important issue to be emphasized is that certain predictions based on these formulas are artefacts, which preclude an adequate interpretation of valuable experimental findings.

The remaining part of this paper is organized as follows. In Section II, the Simmons approach will be reviewed, emphasizing its limitation. The confinement of electron motion in transverse directions, an aspect which is important for nanojunctions with atomic contacts but is not accounted for within the Simmons approach, will be considered in Section III. Section IV is devoted to the comparison of the results for V_t obtained by solving the Schrödinger equation exactly with those of the “exact” WKB and (“approximate” WKB-type) Simmons approach, which clearly demonstrates that the last approach is inappropriate to account for image effects at sizes of interest for nanotransport. In Section V, the case of electrodes with different work functions will be analyzed. An important technical issue, the relationship between the apparent barrier height and the electrodes’ work function, will be addressed in Section VI. Based

on the present exact results for V_t , in Section VII it will be shown that the validity of the WKB approximation has been too optimistically assessed in previous studies. The main results of the present study will be summarized in Section VIII, where possible sources for the disagreement between the present theory and experiment will be indicated.

II. REVIEWING THE SIMMONS’ APPROACH

The theoretical framework of the single-particle tunneling through an energy barrier was established long ago by Sommerfeld.² The current density due to the (elastic) tunneling along the x -direction across a sandwich consisting of an insulating film placed between two (source and drain) electrodes caused by a bias $V > 0$ between source (chosen below as the negative electrode) and drain (positive electrode) with chemical potentials $\mu_S = 0$ and $\mu_D = -eV$ can be expressed as^{2,8,26,29–32}

$$J = 2 \frac{e}{h^3} \int_{\mu_D < E_{\mathbf{p}} < \mu_S} \frac{\partial E_{\mathbf{p}}}{\partial p_x} \mathcal{T}(p_x, V) d^3 \mathbf{p} = \frac{4\pi m e}{h^3} (1) \\ \times \left[eV \int_{-\varepsilon_F}^{-eV} \mathcal{T}(E_x, V) dE_x - \int_{-eV}^0 E_x \mathcal{T}(E_x, V) dE_x \right], (2)$$

where \mathcal{T} is the transmission coefficient. To get Eq. (2), we assumed a parabolic conduction band dispersion $E_{\mathbf{p}} = \frac{1}{2m} (p_x^2 + p_y^2 + p_z^2) - \varepsilon_F$.

To deduce the current, a very popular approach is to employ the WKB expression of the transmission

$$\mathcal{T}_{WKB}(E_x, V) \equiv e^{-\frac{2\sqrt{2m}}{\hbar} \int_{\phi_B(x) > E_x} dx \sqrt{\phi_B(x) - E_x}}. (3)$$

Like many others (e. g., Refs. 1,2,26,29,30,32), Simmons⁸ did not use the above “exact” WKB approximation, but rather an approximate version of the “exact” WKB expression

$$\mathcal{T}_r(E_x, V) = \exp\left(-A\sqrt{\bar{\varepsilon}_B - E_x}\right), (4)$$

replacing the general position dependent barrier $\phi_B(x)$ by a rectangular barrier. In Eq. (4), the fact that the barrier $\phi_B(x)$ is not rectangular is accounted for by considering an effective (average) rectangular barrier of height $\bar{\varepsilon}_B$ and a spatial extension Δs that can be smaller than the distance between electrodes (embedded molecule/nanogap size) d as well as a correction factor γ . This factor enters the quantity $A \equiv 2\gamma\Delta s(2m)^{1/2}/\hbar$. For certain insulating thin films, Simmons estimated $\gamma \simeq 1$ within at most a few percents. A correction factor $\gamma \equiv 1$ has been implicitly assumed in Refs. 9,11 although several earlier studies drew attention on the fact that this assumption is inconsistent with experimental I - V -data for molecular transport. Alternatively, in view of the above expression of A , departures from a rectangular-shaped barrier^{2,8,26} can be considered by employing an effective mass $m^* \neq m$ ($m \rightarrow m^* = m\gamma^2$).^{16,17}

By using Eq. (4), Eq. (2) can be integrated exactly in closed analytical form. The resulting, rather lengthy expression was given previously by various authors (e. g., Refs. 2,26) including Simmons,⁸ who only retained the leading terms in his numerical calculations. The central result of the Simmons approach⁸ is the following expression of the current density J

$$\begin{aligned} J/J_0 = & \bar{\varepsilon}_B \left\{ 1 + \mathcal{O} \left[\left(A\bar{\varepsilon}_B^{1/2} \right)^{-1} \right] \right\} e^{-A\bar{\varepsilon}_B^{1/2}} - (\bar{\varepsilon}_B + eV) \\ & \times \left\{ 1 + \mathcal{O} \left[\left(A(\bar{\varepsilon}_B + eV)^{1/2} \right)^{-1} \right] \right\} e^{-A(\bar{\varepsilon}_B + eV)^{1/2}} \\ & + \mathcal{O} \left[e^{-A(\bar{\varepsilon}_B + \varepsilon_F)^{1/2}} \right], \end{aligned} \quad (5)$$

where $J_0 \equiv e/\hbar/(2\pi\gamma\Delta s)^2$. Eq. (5) applies if the Fermi level of (say,) the right electrode lies above the bottom of the left electrode, $0 < eV < \varepsilon_F$; otherwise the second term in the RHS (“backward” current) should be omitted. This V -range suffices for practical purposes, since it is much broader than the range of the biases, which the molecular junctions fabricated so far can withstand or those used in experiments on vacuum nanojunctions.¹¹ Simmons’ leading order expression (5) was utilized in a series of more recent works^{4-7,10,16,17,19,33} to interpret a series of valuable experimental findings. An important pragmatical advantage of the approaches based on Eqs. (4) and (5) is that it can also simply account for image effects, see Eq. (8).^{2,8,26}

By supposing identical electrodes (work functions $W_S = W_D = W$) first, the total barrier $\phi_B(x)$ through which electrons have to tunnel can be expressed as^{2,31,34}

$$\phi_B(x) = \varepsilon_B - eVx/d + \phi_i(x). \quad (6)$$

In addition to a bare (rectangular) energy barrier ε_B ($\varepsilon_B = W$ for vacuum tunneling), the energy barrier comprises the contributions of the applied bias V and of the charge images $\phi_i(x)$.²

The effective barrier width $\Delta s \equiv s_2 - s_1$ is determined by Simmons from the barrier extension ($0 \leq s_1 < x < s_2 \leq d$) at the electrodes’ Fermi energy without bias (notice that energies are measured throughout relative to the Fermi level)

$$\phi_B(x)|_{x=s_{1,2}} = 0. \quad (7)$$

The effective barrier height is expressed as

$$\bar{\varepsilon}_B = \varepsilon_B - eV \frac{s_1 + s_2}{2d} + \int_{s_1}^{s_2} \frac{dx}{\Delta s} \phi_i(x). \quad (8)$$

In the range of experimental interest ($e|V| < \varepsilon_B$) and ignoring image effects ($\phi_i \equiv 0$), the barrier is trapezoidal, $s_1 = 0$, $\Delta s = s_2 = d$, and $\bar{\varepsilon}_B = \varepsilon_B - eV/2$.

For infinite planar electrodes placed at $x = 0$ and $x = d$, the electrostatic interaction energy $\phi_i(x)$ between an electron located at x and its images can be expressed exactly²

$$\phi_i(x) = \frac{e^2}{4\kappa_r d} \left[-2\psi(1) + \psi\left(\frac{x}{d}\right) + \psi\left(1 - \frac{x}{d}\right) \right], \quad (9)$$

where ψ is the digamma function. To better understand the later analysis, we include throughout a dielectric constant κ_r although for vacuum ($\kappa_r \equiv 1$) it is superfluous. In order to work out Eqs. (7) and (8) in closed analytic forms, various parabolic approximations of the RHS of Eq. (9) around its maximum at $x = d/2$, $\phi_i(d/2) = -\frac{e^2}{\kappa_r d} \log 2$ were employed in Refs. 2,26,29. Instead of Eq. (9), Simmons used the “approximate” expression

$$\phi_i^S(x) \approx -1.15 \log 2 \frac{e^2}{2\kappa_r} \left(\frac{1}{x} + \frac{1}{d-x} \right), \quad (10)$$

which he deduced from his “exact” expression

$$\phi_i^S(x) = -\frac{e^2}{\kappa_r} \left\{ \frac{1}{2x} + \sum_{n=1}^{\infty} \left[\frac{nd}{(nd)^2 - x^2} - \frac{1}{nd} \right] \right\}. \quad (11)$$

In fact, Simmons’ “exact” expression (11) is incorrect. The series entering the RHS of Eq. (11) can be summed out, and the result is twice the RHS of Eq. (9). An easy way to understand this wrong factor is to consider situations very close to one electrode, e. g., $x \gtrsim 0$; then, Eq. (11) yields $\phi_i(x) \simeq -e^2/(2\kappa_r x)$. This is twice the result well known from electrostatics textbooks; the attractive force between a point charge e placed at $x > 0$ and an infinite plane at origin is $F_x(x) = -e^2/(4\kappa_r x^2)$, and the corresponding interaction energy is $\phi_i(x) = -\int_{\infty}^x d\xi F_x(\xi) = -e^2/(4\kappa_r x)$. Simmons’ exact expression misses nothing but the “famous” 1/2 factor related to the fact that the image interaction energy $\phi_i(x)$ is a self energy and not the charge-potential product.³⁵

Recently, Simmons’ expression (10) has been taken over in studies on image effects on the transition voltage.^{9,11} In those works, all the terms (i. e., not only the leading ones written explicitly) in Eq. (5) were used in numerical calculations. To obtain the results presented below referred to as the Simmons results, we have also used these full expressions, as previously done in Refs. 9,11. The terms $\mathcal{O}(\dots)$ which are not explicitly written in Eq. (5) may yield “corrections” to V_t up to $\sim 10\%$,²¹ for smaller values of d and $\bar{\varepsilon}_B$ ($A\bar{\varepsilon}_B^{1/2} \sim 1$). Still, we emphasize that the inclusion of these terms is a priori questionable, as Eq. (5) is basically the result of a (simplified) WKB approximation, and a valid WKB treatment requires sufficiently large values of $A\bar{\varepsilon}_B^{1/2}$ (see Ref. 36 and the discussion below).

As a curiosity, we note that in order to improve the agreement between the theory based on the Simmons approach and the experimental data for vacuum tunneling, a correction factor $\zeta \sim 0.4 - 0.7$ multiplying the RHS of Eq. (10) has been empirically introduced in Ref. 11. It would be tempting to identify ζ with the aforementioned factor 1/2 missing in Eqs. (11) and (10). Unfortunately, the remedy of the Simmons results is not so simple, as it will be shown below.

Let us summarize the basic features of the Simmons’ approach:

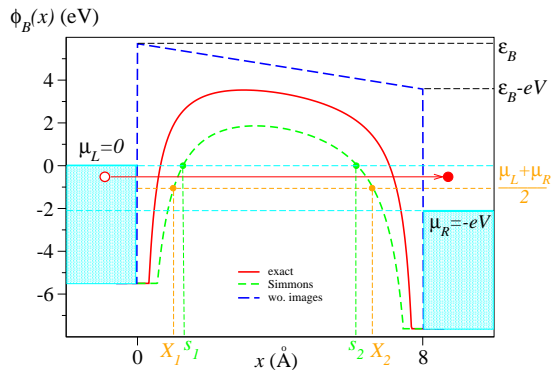


FIG. 1: Energy barrier $\phi_B(x)$ for $\varepsilon_B \equiv W = 5.7$ eV, $d = 8$ Å, and $\kappa_r = 1$ computed using the exact contribution of charge images, Eq. (9), and using the Simmons’ “approximation”, Eq. (10), at $V \equiv V_i = 2.12$ V. Notice that the height and width of the Simmons barrier are substantially smaller than the exact ones, and therefore image effects are drastically overestimated by the Simmons model.

(i) Electrons tunnel across an energy barrier $\phi_B(x)$ in x -direction and move freely in transverse (y , z)-directions, cf. Eq. (1).

(ii) The transmission coefficient across the barrier is computed within an approximation *more* restrictive than the WKB-approximation, which assumes that the barrier profile $\phi_B(x)$ can be replaced by a rectangular effective barrier

$$\int \frac{dx}{\Delta s} \sqrt{\phi_B(x) - E_x} \approx \gamma \sqrt{\bar{\varepsilon}_B - E_x} \approx \sqrt{\bar{\varepsilon}_B - E_x}, \quad (12)$$

where the (E_x - and V -independent) correction factor can be taken $\gamma \simeq 1$. This amounts to consider that, irrespective of their energy ($\mu_D < E_x < \mu_S$), all electrons that contribute to the current tunnel across a barrier of the same width $\Delta s = s_2 - s_1$ and height $\bar{\varepsilon}_B$, which is the barrier “seen” by the electrons at the Fermi level of the unbiased junction ($E_x = 0$), cf. Eqs. (7) and (8), and Fig. 1.

(iii) The contribution of charge images to the energy barrier is estimated from Eq. (10). This overestimates the image effects by a factor ~ 2 .³⁷

To demonstrate the fact that the Simmons approach is inadequate for nanojunctions, we will compare below the results of this approach both with the results of the “exact” WKB approximation [i. e., by using Eq. (3) and not Eq. (4)] as well as with the exact results obtained by solving the Schrödinger equation with the exact barrier potential, Eq. (6). The exact transmission $\mathcal{T}(E_x, V)$ can be easily obtained by imposing the overall continuity of the wave function and its derivative. Inside the junction ($0 < x < d$), the wave function $\Psi(x)$ obeys the Schrödinger equation

$$\left[-\frac{\hbar^2}{2m} \frac{\partial^2}{\partial x^2} + \phi_B(x) - E_x \right] \Psi(x) = 0. \quad (13)$$

The exact Schrödinger equation written above can easily be solved analytically in the absence of images ($\phi_i \equiv 0$).³¹ The exact wave function $\Psi(x)$ for this case can be expressed as a linear combination of the Airy functions $Ai(z)$ and $Bi(z)$, where $z \equiv \zeta - x/\lambda$ and

$$\zeta \equiv \left[\frac{2m^*}{\hbar^2} \left(\frac{d}{eV} \right)^2 \right]^{1/3} (\varepsilon_B - E_x); \quad \frac{1}{\lambda} \equiv \left(\frac{2m^*}{\hbar^2} \frac{eV}{d} \right)^{1/3}.$$

The transmission is given by $\mathcal{T}(E_x, V) = \mathcal{N}(E_x, V)/\mathcal{D}(E_x, V)$, where³¹

$$\mathcal{N} = 4 \frac{k_S k_D}{d^2} (A_D B'_D - A'_D B_D)^2,$$

$$\mathcal{D} = \left[\frac{1}{d^2} (A'_S B'_D - A'_D B'_S) + k_S k_D (A_S B_D - A_D B_S) \right]^2 + \left[\frac{k_S}{d} (A_S B'_D - A'_D B_S) + \frac{k_D}{d} (A_D B'_S - A'_S B_D) \right]^2.$$

Above, the obvious dependence on E_x and V has been omitted for brevity, the subscripts S and D correspond to $x = 0$ and $x = d$, respectively, and the prime stands for the derivative of the Airy functions with respect to z , e. g., $A_D \equiv Ai(\zeta - d/\lambda)$ and $B'_S \equiv [d Bi(z)/dz]_{z=\zeta}$, $k_S \equiv \sqrt{2m(\varepsilon_F + E_x)}/\hbar$, and $k_D \equiv \sqrt{2m(\varepsilon_F + E_x + eV)}/\hbar$.

In the presence of image effects, we have performed exact numerical calculations for the potential given by Eqs. (6) and (9) or (10). To this aim, we used a sufficiently large number N of small pieces (until reaching the convergence) $0 \equiv x_0 \leq x_1 \leq \dots \leq x_N \equiv d$ and considered piecewise constant potentials $\phi_{B,n} = \int_{x_{n-1}}^{x_n} \phi_B(\xi)/(x_n - x_{n-1})$.

III. LATERAL CONFINEMENT

Eq. (5) represented the starting point for interpreting many valuable experimental results for molecular junctions. Therefore, it is noteworthy that, in fact, the description based on Eq. (1), from which Eq. (5) is deduced, is appropriate neither for molecular junctions nor for vacuum nanojunctions with atomic contacts, because in those cases the electron motion transverse to the junction is confined. Rather than being continuous variables ($0 < E_{y,z} < \varepsilon_F$ at zero temperature), the transverse energies are quantized, and only the lowest-energy transverse channel contributes to electric conduction. Therefore, to describe electric transport in such junctions, the integration over the transverse (y , z) directions should be omitted, and the counterpart of Eqs. (1) and (2) is a current expressed by

$$I = 2 \frac{e}{h} \int_{-eV}^0 \mathcal{T}(E_x, V) dE_x. \quad (14)$$

It is worth emphasizing that Eq. (14) qualitatively differs from Eq. (2). To understand that Eq. (2) is basically inappropriate for nanotransport, let us consider the linear

conductance

$$G \propto \lim_{V \rightarrow 0} \frac{dJ(V)}{dV} \propto \int_0^{\varepsilon_F} \mathcal{T}(E_x, V=0) dE_x. \quad (15)$$

Eq. (15) is inconsistent with Landauer’s fundamental statement for the transport at nanoscale (“conductance is transmission”, $G \propto \mathcal{T}(\varepsilon_F, V=0)$). The electrons contributing to Eq. (15) can have a kinetic energy E_x of motion across the junction spanning the whole conduction band ($0 \leq E_x \leq \varepsilon_F$); E_x is not restricted to $E_x \simeq \varepsilon_F$. This is the consequence of the fact that the lateral (y, z) confinement is missing in Eq. (2). The states contributing to linear response in Eq. (1) have a total energy $E_{\mathbf{p}} \equiv E_x + E_y + E_z \simeq \varepsilon_F$, but the transverse kinetic energies are continuous variables in the range $0 < E_{y,z} < \varepsilon_F$. To conclude, Eq. (2) may be appropriate for traditional electronics envisaged by Simmons, but not for nanojunctions with atomic contacts, wherein the lateral confinement is essential and Eq. (14) should be used.

Mathematically speaking, the only difference between the situation without lateral confinement discussed in Section IV and that with lateral confinement is the manner of carrying out the energy integration, namely, Eq. (2) versus Eq. (14). Whether computed exactly by solving the Schrödinger equation (13) or approximately via Eq. (3) or Eq. (4) the transmission coefficient is given by the same formula. This is the main reason why the shortcomings of the Simmons results presented below are essentially the same, irrespective whether the one-dimensional or three-dimensional description, underlying Eqs. (14) or (2), respectively is employed.

IV. SIMMONS’ RESULTS VERSUS WKB AND EXACT RESULTS

In the cases typical for thin dielectric/semiconducting films, with (practically) infinite transverse extension and widths $d \sim 20 - 50 \text{ \AA}$, large dielectric constants $\kappa_r \sim 10$ [cf. Eqs. (9) and (10)], and voltages that are not too high analyzed by Simmons,⁸ the approximations underlying Eq. (5) may be reasonable.

However, we will show that the above approximations are not justified for molecular/nano-junctions. Although we are going to present only results obtained by accounting for the lateral confinement discussed in Section III, we note that there are only insignificant quantitative difference between the exact, WKB, and Simmons results also when the lateral confinement is ignored. To emphasize again, the shortcomings of the Simmons approach discussed in this paper are not specific for the cases where the lateral confinement is important.

To obtain the numerical results presented below, we fixed the Fermi energy to the value $\varepsilon_F = 5.5 \text{ eV}$ specific for gold, employed experimental work function values $W_{S,D} = 3.2 - 5.7 \text{ eV}$ (see also Section VI below), and considered nanogap sizes d relevant for experiments.¹¹

Let us first examine the case of a relatively wide ($d = 8 \text{ \AA}$) vacuum junction ($\kappa_r \equiv 1$) with electrodes characterized by identical work functions $\varepsilon_B = W_S = W_D = 5.7 \text{ eV}$ (i. e., the highest experimental value, which is the most favorable for a valid WKB treatment). The consideration of vacuum nanojunctions obviates an important conceptual issue for molecular junctions. In the latter, in view of the finite tunneling time (τ) spent by electrons within the barrier (“molecule”), it is unclear whether the static dielectric constant $\kappa_r(\omega)|_{\omega=0}$ or the dynamical dielectric $\kappa_r(\omega)|_{\omega \sim 1/\tau}$ should be used in Eq. (9).

Results for the vacuum nanogap specified above are presented in Fig. 2. The lower group of three curves (which can hardly be distinguished among themselves within the drawing accuracy) represent exact, WKB and Simmons results obtained by ignoring image effects. For the bias range of experimental interest ($V \lesssim$

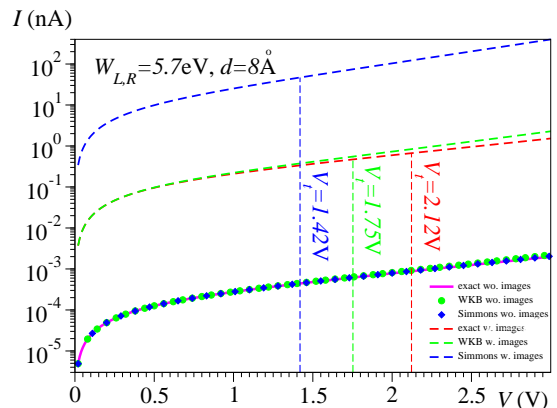


FIG. 2: I - V -characteristics without and with images. Notice that the curve deduced from full quantum-mechanical calculations (label “exact”) without and with images has been multiplied with a factor 0.250 and 0.503, respectively, which represents the deviation of the ohmic conductance of the “exact” WKB value from the “exact” conductance.

3 V),¹¹ ignoring image effects, the Simmons approximation agrees well with the “exact” WKB approximation. Concerning the latter, it basically deviates from the exact quantum-mechanical calculations by a *constant* factor $I_{exact} \simeq 0.250 I_{WKB}$. Although this constant factor precludes a quantitative analysis of experimental I - V -characteristics, it does not notably affect the transition voltage ($V_t = 2.13 \text{ V}$ for the lower group of curves without images in Fig. 2), deduced from the minimum of $\log(I/V^2)$ ($= \log I - 2 \log V$). For the highest work function $W_S = W_D = 5.7 \text{ eV}$ deduced in experiments,¹¹ a difference $\delta V_t \simeq 0.1 \text{ V}$ (comparable to the experimental inaccuracy^{4,19,23}) from the approximate estimates and the exact value sets the smallest nanogap size $d_{min} \simeq 8 \text{ \AA}$ for reliable WKB and Simmons approximations for this case. Briefly, the Simmons (and WKB) approximation yields reasonable estimates of the transition voltage V_t for barriers sufficiently high and wide *if* image effects were

negligible. However, this situation deteriorates at smaller sizes (see Fig. 3a) and heights even without charge images.

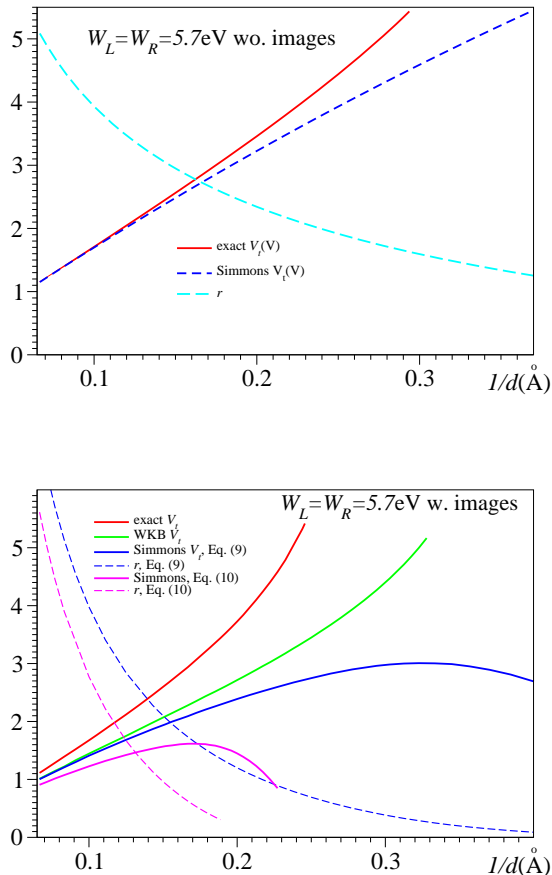


FIG. 3: Exact, WKB, and Simmons results on the transition voltage for vacuum tunneling (a) without and (b) with charge images. In the latter case, results obtained within the Simmons approach are shown both with the incorrect and with the correct image forces [Eqs. (10) and (9), respectively]. The curves for $r \equiv A\bar{\epsilon}_B^{1/2}/4$ reveal that the condition $r > 1$ of Ref. 36 for a valid WKB approximation is too optimistic.

The situation drastically changes when image effects are considered. Because they rounds off the barrier corners, diminish and narrows the barrier hill,² image effects increase the tunneling current. Image effects are most pronounced in vacuum (lowest $\kappa_r = 1$). For the case of Fig. 2, the exact current is enhanced by three orders of magnitude. Due to the incorrect factor in Eq. (11) image effects are drastically exaggerated by the Simmons approach. The example of Fig. 2 demonstrates that not only the Simmons results, but also the WKB values significantly deviate from the exact ones. They become unacceptable at the relatively large barrier widths and heights at which they would be reasonable without image effects. This holds true not only for the magnitudes of the currents, but also for the values estimated for the transi-

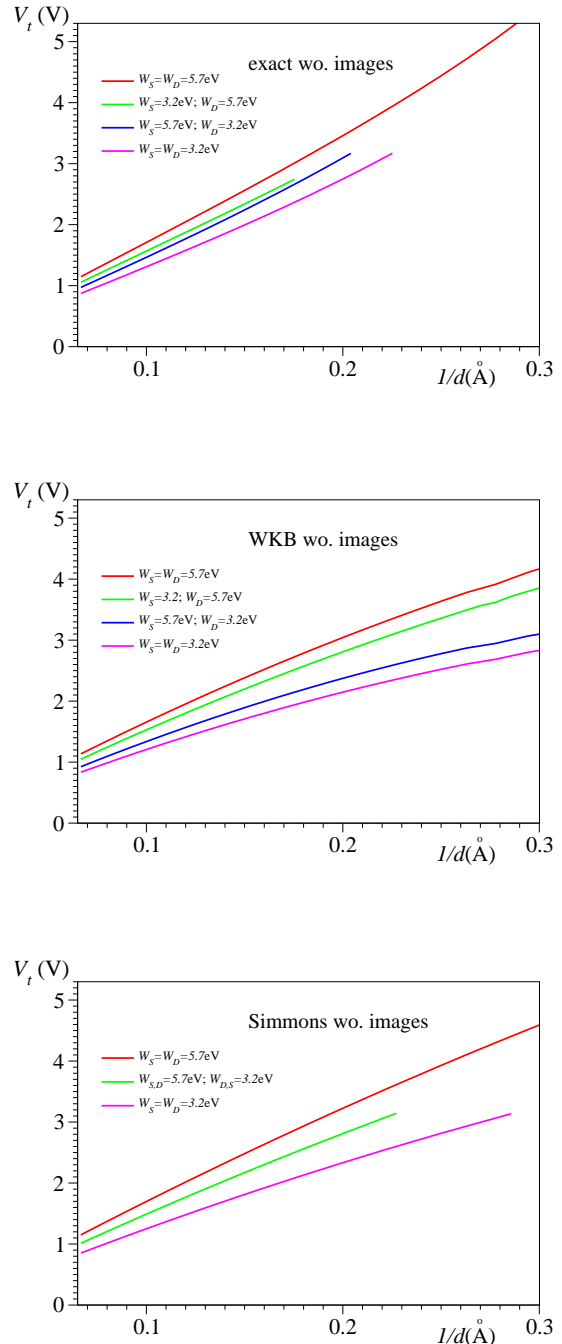


FIG. 4: Transition voltage for vacuum tunneling without images computed exactly, and within the WKB and Simmons methods for electrodes with equal and different work functions $W_{S,D}$ specified in the legend. Without image effects, the Simmons curves for $(W_S = 5.7 \text{ eV}, W_D = 3.2 \text{ eV})$ and $(W_S = 3.2 \text{ eV}, W_D = 5.7 \text{ eV})$ coincide. Notice that, with our choice, the source/drain (S/D) is the negative/positive electrode and V_t -values are always positive.

tion voltage. This is illustrated by the exact, WKB and Simmons results for the transition voltage in the pres-

ence of charge images, which are presented in Figs. 3b and 4. As visible there, Simmons' estimates for V_t are acceptable only for large sizes ($d > 20 \text{ \AA}$) where image effects are negligible altogether.

Still, this is not the whole issue concerning the validity of the Simmons model in cases where image effects are significant. Most importantly, the Simmons approach even yields a *qualitatively* incorrect prediction. This fact becomes clear by inspecting the curves depicted in Fig. 3b, and by comparing the panels of Fig. 5 among themselves. As visible there, the Simmons curves are qualitatively incorrect; they exhibit a maximum, which the exact curves do not display. The trend toward smaller sizes is just opposite: while, roughly, V_t is inversely proportional to d at large sizes in both cases, at low sizes the exact V_t -values increase superlinearly with $1/d$ whereas the Simmons estimates decrease with $1/d$. Simmons curves exhibiting a maximum have been previously shown in Refs. 9,11, where the three-dimensional description [Eq. (2)] was implicitly assumed. The present comparison with the exact curves demonstrates that this maximum is nothing but an artefact of the Simmons approximation, and this applies irrespective whether a lateral confinement is accounted for or not. The occurrence of this Simmons maximum for curves of $V_t(d)$ is an artefact of the WKB rectangular-barrier approximation [approximation (ii) of Section II], while the fact that this maximum is located at such small sizes is the consequence of the incorrect factor of Eqs. (11) and (10) (as noted under (iii) in Section II). Computations based on the approximate transmission given by Eq. (4) using the image potential energy of Eq. (9) instead of Eq. (10) still yield a maximum in $V_t(d)$ albeit located at substantially smaller sizes. This fact is illustrated by Figs. 3b, and 5c,d.

V. ASYMMETRY DRIVEN BY DIFFERENT ELECTRODES' WORK FUNCTIONS

So far, we have considered electrodes characterized by identical work functions ($W_S = W_D$). This is a reasonable assumption for vacuum tunneling between planar crystalline electrodes with macroscopic transverse extensions consisting of the same metal (even) if their separation (d) falls in the nanometer range. However, this is an unlikely situation in molecular/nano-electronics with atomic contacts. Even for electrodes of the same chemical nature (e. g., gold), it is unlikely that the local crystal orientation at contacts, which is hard to control experimentally, is identical. This general feature has been confirmed by the experimental data from the vacuum tunneling junctions fabricated in Ref. 11, for which values $W \sim 3.2 - 5.7 \text{ eV}$ have been deduced (see also Section VI below). This fact strongly supports the idea that not only the work functions characterizing different junctions are different, but also the values characterizing the (say,) left and right electrodes of a *given* junction can be dif-

ferent. This effect seems to be not properly considered in recent studies on nanoelectronic devices with atomic contacts, but may be quite relevant, as already pointed out by Sommerfeld [see Ch. 20(b) and Fig. 36 of Ref. 2].

In the case of electrodes with different work functions ($W_S \neq W_D$), a nonvanishing Volta potential difference arises, which yields an intrinsic (Volta) field $(W_D - W_S)/(ed)$ that favors the motion of electrons from the metal with the higher work function to that with the lower work function.² In such situations, the above Eq. (6) should be generalized to express the total barrier $\phi_B(x)$ to account for the Volta field as follows^{2,31,34}

$$\phi_B(x) = \varepsilon_B + (W_D - W_S - eV)x/d + \phi_i(x). \quad (16)$$

It is worth emphasizing that the Volta field is significant: the above example reveals that values of $W_D - W_S$ can be a few electronvolts, such that the Volta field can be even larger than the applied field, since molecular/nano-junctions can hardly withstand voltages larger than $V \sim 2 - 3 \text{ V}$.^{11,19,38}

More or less asymmetric experimental I - V -characteristics for positive and negative biases [i. e., $I(V) \neq -I(-V)$] are ubiquitous in the transport at nanoscale. This is also the case of the vacuum nano-junctions of Ref. 11. A consequence of this symmetry breaking is the fact that the transition voltages for positive and negative biases V are different, a fact clearly visible in Fig. 1 of Ref. 11.

One can easily convince oneself that the I - V -characteristics deduced from Eqs. (6), (14) [or (1)] by using the barrier (6) are symmetric, $I(V) = -I(-V)$. As a consequence, the transition voltages deduced for positive and negative biases are of equal magnitude. However, this symmetry becomes broken in the cases where the work functions are different. As an illustration of this asymmetry, in Figs. 4 and 5, we present results obtained by employing the experimental values of the work functions $\{W_S, W_D\} = \{5.7, 3.2\} \text{ eV}$ mentioned above, both by considering and ignoring image effects. The curves for the transition voltages computed exactly exhibit the aforementioned asymmetry both without and with charge images, in qualitative agreement with experiment.

The work function asymmetry ($W_S \neq W_D$) can represent a general source for asymmetric I - V -characteristics for nanojunctions and even for devices based on symmetric molecules. In molecular devices, it can further enhance the asymmetry of the electric potential profile obtained by solving the Poisson-Schrödinger equations selfconsistently.

As in the case of identical electrodes, the Simmons curves for V_t are unacceptable. By ignoring image effects, the Simmons curves are not asymmetric (cf. Fig. 4c), while by considering image effects all these curves exhibit a maximum (cf. Fig. 5c), which is absent for the exact curves and is nothing but an artefact of an inadequate approximation.

VI. APPARENT BARRIER HEIGHT VERSUS WORK FUNCTION

In the calculations presented above we have employed the (extreme) values of the work functions $W_{S,D}$ (3.2 eV and 5.7 eV) given in Ref. 11. These values have been deduced there from tunneling conductance G measurements by assuming a dependence $G \propto \exp(-2d\sqrt{2m\Delta}/\hbar)$ at larger d ,³⁹ and identifying the apparent barrier height Δ with W . In Fig. 6, we present results for the conductance computed exactly with and without charge images. In the absence of image effects, the curves $G(d)$ demonstrate a virtually perfect exponential decay down to $d \rightarrow 0$ and the deduced apparent height is $\Delta = \overline{W} \equiv (W_S + W_D)/2$. By including the image forces, an exponential decay is still visible at larger d . However, at smaller d -values deviations from the exponential decay are clearly visible, which set in the faster, the lower the work functions are. The apparent height deduced from the large- d portion is no more equal to the average work function, $\delta\Delta \equiv \Delta - \overline{W} \neq 0$. From our exact numerical data, we found a difference $\delta\Delta$, which does not depend on $W_{S,D}$ and amounts $\delta\Delta \simeq -0.57$ eV. To further check that this difference is a genuine image effect, we also performed similar calculations by artificially increasing the dielectric constant κ_r from the vacuum value ($\kappa_r \equiv 1$). In agreement with the presence of κ_r in the denominator of the RHS of Eq. (9), we deduced from our numerical results a virtually perfect scaling $\delta\Delta(\kappa_r) \simeq -0.57$ eV/ κ_r .

Our exact numerical results indicate that even in the presence of image forces, the work function asymmetry $\delta W \equiv W_S - W_D \neq 0$ has practically no effect on the linear tunneling conductance; it solely depends on the average value \overline{W} . In contrast to the case at high voltages, the most exotic asymmetric values of $W_{S,D}$ can hardly change the linear conductance by one percent, so we can safely ignore this effect at low voltages V . Still, this behavior indicates that the linear conductance data do not suffice, and a further refinement is needed to estimate the values of $W_{S,D}$ from the experimental data.

Attempting to undertake this effort seems to make little sense at present. Although relatively large, the above $\delta\Delta$ -value is still smaller than the experimental inaccuracy of ~ 1 eV of the apparent barrier heights deduced in Ref. 11. Therefore, in our numerical calculations, we have simply taken over the experimental values $W_{S,D} = 3.2; 5.7$ eV deduced without applying corrections due to the fact that $\delta\Delta \neq 0$ and $\delta W \neq 0$.

VII. ON THE VALIDITY OF THE WKB METHOD

The results for the transition voltage presented above showed that, qualitatively, the "exact" WKB curves for V_t behave similar to the exact ones; quantitatively, differences at smaller sizes are significant. Concerning the WKB method, we make the following comment at this

point. The exact counterpart of Eq. (4), the transmission through a rectangular barrier hill ($\overline{\varepsilon}_B > E_x$) is well known

$$\begin{aligned} \mathcal{T}(E_x, V) = & 4k_S k_D \kappa_B^2 / \left[\kappa_B^2 (k_S + k_D)^2 \cosh^2(\kappa_B s) \right. \\ & \left. + (k_S k_D - \kappa_B^2)^2 \sinh^2(\kappa_B s) \right], \end{aligned} \quad (17)$$

where $\kappa_B \equiv [2m(\overline{\varepsilon}_B - E_x)]^{1/2}/\hbar$ and $k_{S,D}$ have been defined above. [Notice that for rectangular barriers, the Simmons and WKB expressions coincide, cf. Eqs. (3) and (4).] Based on the fact that $\cosh z \approx \sinh z \approx \exp(z)/2$ for large z , it was claimed that the WKB results should not notably differ from the exact ones if³⁶

$$r \equiv A\sqrt{\overline{\varepsilon}_B}/4 \gtrsim 1. \quad (18)$$

However, by inspecting the curves for r in Fig. 3, one must conclude that Eq. (18) does not guarantee reliable WKB and Simmons estimates for V_t . Although the hyperbolic functions entering Eq. (17) reduce to an exponential for large arguments, there still remains an important difference between the exact and WKB transmission, namely the preexponential factor, which is energy- and V -dependent. Were this factor constant, $I_{WKB} = \text{const} \times I_{\text{exact}}$, the WKB and exact FN-curves $\log(I_{WKB}/V^2) = \log(I_{\text{exact}}/V^2) + \text{const}$ would have the minima at the same (transition-)voltage, but our results of Figs. 3, 4, and 5 contradict that V_t^{WKB} represents a reliable estimates for V_t^{exact} . So, the folkloristic dictum on a slowly varying prefactor multiplying a rapidly varying exponential does not hold for cases of interest in molecular/nano-transport. The need to reconsider the prefactor in the FN-tunneling theory for field-emission, a topic of traditional vacuum electronics, has also been pointed recently.⁴⁰ As is well known from textbooks, the validity of the WKB approximation is difficult to assess in general. Conclusive evidence only comes from the direct comparison with the exact results, largely rendering the WKB calculations superfluous.

Although the WKB curves for V_t can significantly deviate from the exact ones, at least they are qualitatively correct; they do not exhibit the spurious maximum of the Simmons curves. Therefore, one may still ask what is the key difference between the the WKB and Simmons approximations. In the latter, the actual barrier $\phi_B(x)$ is replaced by a *rectangular* barrier, and this comprises two aspects. A rectangular barrier does not only mean a constant height $\overline{\varepsilon}_B$ [as if the potential drops at the contacts were the same (namely, $V/2$)], but also a constant (energy-independent) barrier width $s = s_2 - s_1$, cf. Eq. (7). Let us examine Fig. 1. Within the WKB method, depending on their energy, the electrons with energies in the Fermi window ($\mu_S = 0 > E_x > \mu_D = -eV$) that contribute to the tunneling current "see" a barrier $\phi_B(x) - E_x$ whose width $x_2(E_x) - x_1(E_x)$ is E_x -dependent. Here, $x_{1,2}$ are defined by $\phi_B(x_{1,2}) = E_x$. Within the Simmons approximation, electrons tunnel across a rectangular barrier $\overline{\varepsilon}_B - E_x$ whose width $\Delta s =$

$s_2 - s_1$ is the smallest; $x_1(E_x) \leq s_1$ and $x_2(E_x) \geq s_2$. Practically, all electrons that contribute to the WKB-current tunnel through a barrier broader than the Simmons barrier, and this is the most important reason why the Simmons method (even letting alone the missing factor $1/2$) overestimates the image effects. The approximation $x_2(E_x) - x_1(E_x) \approx s_2 - s_1$ may be justifiable for low biases ($\mu_S - \mu_D = eV \ll \varepsilon_B$), but at higher biases the width of the effective barrier is significantly larger than $s_2 - s_1$. As a remedy, one can determine the effective width by using the barrier midway between μ_S and μ_D , i. e., using $\phi_B(x)|_{x=X_{1,2}} = (\mu_S + \mu_D)/2 = -eV/2$ instead of Eq. (7). This attempt is a trade off of enhanced (reduced) tunnel probabilities of electron states below (above) the orange line of Fig. 1, which wipes out the spurious maximum of the Simmons curves discussed above, but it still represents an approximate treatment more restrictive than the “exact” WKB approximation of Eq. (3).

VIII. SUMMARY AND OUTLOOK

The results reported in the present paper can be summarized as follows:

(i) We have drawn attention on the fact that the utilization of the barrier picture for molecular or nano-junctions with atomic contacts should properly account for the confinement of the transverse electron motion, a feature not included into the Simmons formula (5).

(ii) We have presented a detailed comparison of the results for the transition voltage obtained exactly and within the Simmons model. Particular emphasis has been laid on the fact that the Simmons method, whose formulas have been utilized to process valuable experimental data in several recent studies, is inadequate for molecular/nano-junctions. Letting alone that the Simmons model (a) ignores the transverse confinement, (b) it drastically overestimates the image effects because of the missing factor $1/2$ in the employed expression of the image interaction energy, and (c) predicts a spurious maximum in the curve for $V_t(d)$, which is an artefact of a specific rectangular barrier approximation.

(iii) We have presented results demonstrating that, as far as the transition voltage is concerned, the validity of the WKB method was too optimistically assessed previously.

(iv) We have discussed that a nonvanishing difference between the electrodes’ work functions, which is likely the case in most experimental setups based on atomic contacts, may be significant for the ubiquitous asymmetry of the I - V -characteristics and the different V_t -magnitudes at opposite bias polarities.

Despite intensive and extensive theoretical and experimental efforts in the last decade, the field of molecular transport is still confronted with a series of difficulties. The transport problem is alleviated when electrons tunnel through a vacuum nanogap, and one needs no more to

consider, e. g., how the positions and widths of the molecular levels change upon contacting to electrodes, what is the role played by molecular correlations, what is the potential profile across the embedded molecule, *etc.*, and all these in a nonequilibrium current-carrying state. Therefore, aiming to gain further insight into the transport at nanoscale by (also) studying vacuum nanojunctions, as recently done experimentally,¹¹ appears as a noteworthy attempt.

Although, for reasons like those enumerated above, the transport through vacuum nanogaps should be easier to understand, it turns out to be far from trivial. The present study demonstrates that the curves of $V_t = V_t(d)$ reported for the vacuum nanojunctions investigated experimentally in Ref. 11 are rather challenging. In the present paper, we have demonstrated that the initial tentative attempt to explain the weak and broad maximum (almost a broad plateau) of the experimental $V_t(d)$ -curves within Simmons-type calculations¹¹ (letting alone that the Simmons maxima are much more pronounced and narrow than the experimental ones) cannot be justified; the computed maxima turn out to be an artefact of the Simmons approach. While being able to indicate the drawbacks of the Simmons approach, we could not explain the weak d -dependence of the experimental curve for V_t , although our results for $V_t(d)$ have been obtained by solving the Schrödinger equation (13) *exactly* and employing the expression (9) of the charge image contribution, an *exact* result of classical electrostatics. The weakly d -dependent experimental values of V_t , which fall in range $\sim 1.5 - 2.5$ V (depending on the apparent barrier height) for $d \lesssim 8 \text{ \AA}$ ¹¹ are significantly smaller than the theoretical estimates of Fig. 5a. This clearly indicates that other effects, not included within our treatment, should be considered, and in the following we will enumerate several possibilities.

Since the “exact” Eq. (9) applies to the case of infinite planar electrodes, described as classical continuous media rather than atomic arrays, one could attempt to employ a more realistic geometry, or to consider effective image planes at $x = x_0$ and $x = d - x_0$ (with $x_0 \sim 2 \text{ \AA}$), displaced from the nominal surfaces at $x = 0$ and $x = d$, as suggested from intuitive reasons² or by LDA-calculations.⁴¹ The classical result expressed by Eq. (9) can be deduced microscopically as an effect of surface plasmons in metallic electrodes.⁴² By considering the static limit ($\omega \rightarrow 0$) of the surface plasmon polarization, one obtains deviations from Eq. (9)

$$\begin{aligned} \phi_i(x) = & \frac{e^2}{4\kappa_r d} \left[B_u\left(\frac{x}{d}, 0\right) + B_u\left(1 - \frac{x}{d}, 0\right) + 2\log(1 - u) \right. \\ & \left. - \psi\left(\frac{x}{d}\right) - \psi\left(1 - \frac{x}{d}\right) + 2\psi(1) \right] \end{aligned}$$

where $u \equiv \exp(-2k_c d)$, k_c being a surface plasmon momentum cutoff, and B is the incomplete beta function.⁴² Eq. (9) can be obtained from the above equation by taking the (“local”) limit $k_c \rightarrow \infty$. Retardation effects ($\omega \neq 0$) due to local phonons, surface plasmons^{42,43} or

finite tunneling time⁴⁴ could also play an important role. Last but not least, in view of the well known fact that the image potential can bind electrons near the surface of liquid helium,⁴⁵ surface image electron states should also deserve consideration. A possible role of electron states localized at electrode's surface has already been suggested in Ref. 11 and discussed more quantitatively in Ref. 23.

Acknowledgment

The financial support for this work provided by the Deutsche Forschungsgemeinschaft (DFG) is gratefully acknowledged.

-
- * Also at National Institute for Lasers, Plasma, and Radiation Physics, ISS, POB MG-23, RO 077125, Bucharest, Romania
- ¹ A. Sommerfeld, *Z. Phys.* **47**, 1 (1928).
 - ² A. Sommerfeld and H. Bethe, *Handbuch der Physik*, edited by Geiger and Scheel, volume 24, page 446, Julius-Springer-Verlag, 1933.
 - ³ A. Aviram and M. A. Ratner, *Chem. Phys. Lett.* **29**, 277 (1974).
 - ⁴ J. M. Beebe, B. Kim, J. W. Gadzuk, C. D. Frisbie, and J. G. Kushmerick, *Phys. Rev. Lett.* **97**, 026801 (2006).
 - ⁵ S. Ho Choi, B. Kim, and C. D. Frisbie, *Science* **320**, 1482 (2008).
 - ⁶ J. M. Beebe, B. Kim, C. D. Frisbie, and J. G. Kushmerick, *ACS Nano* **2**, 827 (2008).
 - ⁷ B. Kim, J. M. Beebe, Y. Jun, X.-Y. Zhu, and C. D. Frisbie, *J. Amer. Chem. Soc.* **128**, 4970 (2006).
 - ⁸ J. G. Simmons, *J. Appl. Phys.* **34**, 1793 (1963).
 - ⁹ E. H. Huisman, C. M. Guedon, B. J. van Wees, and S. J. van der Molen, *Nano Letters* **9**, 3909 (2009).
 - ¹⁰ S. H. Choi et al., *J. Amer. Chem. Soc.* **132**, 4358 (2010).
 - ¹¹ M. L. Trouwborst et al., *Nano Letters* **11**, 614 (2011).
 - ¹² M. Araidai and M. Tsukada, *Phys. Rev. B* **81**, 235114 (2010).
 - ¹³ J. Chen, T. Markussen, and K. S. Thygesen, *Phys. Rev. B* **82**, 121412 (2010).
 - ¹⁴ T. Markussen, J. Chen, and K. S. Thygesen, *Phys. Rev. B* **83**, 155407 (2011).
 - ¹⁵ I. Báldea, *Chem. Phys.* **377**, 15 (2010).
 - ¹⁶ R. E. Holmlin et al., *J. Amer. Chem. Soc.* **123**, 5075 (2001).
 - ¹⁷ W. Wang, T. Lee, and M. A. Reed, *J. Phys. Chem. B* **108**, 18398 (2004).
 - ¹⁸ P.-W. Chiu and S. Roth, *Appl. Phys. Lett.* **92**, 042107 (2008).
 - ¹⁹ H. Song et al., *Nature* **462**, 1039 (2009).
 - ²⁰ H. Song, Y. Kim, H. Jeong, M. A. Reed, and T. Lee, *J. Phys. Chem. C* **114**, 20431 (2010).
 - ²¹ A. J. Bergren, R. L. McCreery, S. R. Stoyanov, S. Gusarov, and A. Kovalenko, *J. Phys. Chem. C* **114**, 15806 (2010).
 - ²² H. Song, M. A. Reed, and T. Lee, *Adv. Mater.* **23**, 1583 (2011).
 - ²³ M. C. Lennartz, N. Atodiresei, V. Caciuc, and S. Karthaeuser, *J. Phys. Chem. C*, doi: 10.1021/jp204240n.
 - ²⁴ R. H. Fowler and L. Nordheim, *Proc. Roy. Soc. London A* **119**, 173 (1928).
 - ²⁵ L. W. Nordheim, *Proc. Roy. Soc. London A* **121**, 626 (1928).
 - ²⁶ R. Holm, *J. Appl. Phys.* **22**, 569 (1951).
 - ²⁷ J. Bardeen, *Phys. Rev. Lett.* **6**, 57 (1961).
 - ²⁸ W. A. Harrison, *Phys. Rev.* **123**, 85 (1961).
 - ²⁹ R. Stratton, *J. Phys. Chem. Solids* **23**, 1177 (1962).
 - ³⁰ T. E. Hartman, *J. Appl. Phys.* **35**, 3283 (1964).
 - ³¹ K. H. Gundlach, *Solid-State Electronics* **9**, 949 (1966).
 - ³² W. F. Brinkman, R. C. Dynes, and J. M. Rowell, *J. Appl. Phys.* **41**, 1915 (1970).
 - ³³ V. B. Engelkes, J. M. Beebe, and C. D. Frisbie, *J. Amer. Chem. Soc.* **126**, 14287 (2004).
 - ³⁴ J. G. Simmons, *J. Appl. Phys.* **34**, 2581 (1963).
 - ³⁵ A. Hartstein, Z. A. Weinberg, and D. J. DiMaria, *Phys. Rev. B* **25**, 7174 (1982).
 - ³⁶ K. Gundlach and J. Simmons, *Thin Solid Films* **4**, 61 (1969).
 - ³⁷ The factor 1.15 entering Eq. (10) represents an empirical correction, which makes the “approximate” average value closer to the “exact” one. Without this factor, the maximum values obtained from Eq. (11) and Eq. (10) coincide [$\phi_i(x = d/2) = -2e^2 \log 2 / (\kappa_r d)$], but near electrodes ($x \gtrsim 0$ and $x \lesssim d$) the “approximate” values given by the latter equation are smaller than the “exact” values given by the former equation. A significantly better approximation than Eq. (10), which recovers the exact results in the limits $x \gtrsim 0$, $x \approx d/2$, and $x \lesssim d$ is⁴² $\phi_i(x) \approx -\frac{e^2}{4\kappa_r} \left(4 \frac{\log 2 - 1}{d} + \frac{1}{x} + \frac{1}{d-x} \right)$.
 - ³⁸ Notice, however, that the Volta field only affects the energy barrier and not the integration limits in Eqs. (1) and (14).
 - ³⁹ G. Binnig, N. Garcia, H. Rohrer, J. M. Soler, and F. Flores, *Phys. Rev. B* **30**, 4816 (1984).
 - ⁴⁰ R. G. Forbes, *J. Appl. Phys.* **103**, 114911 (2008).
 - ⁴¹ N. D. Lang and W. Kohn, *Phys. Rev. B* **7**, 3541 (1973).
 - ⁴² Z. Lenac and M. Sunjic, *Nuovo Cimento B* **33**, 681 (1976).
 - ⁴³ A. Tagliacozzo and E. Tosatti, *Physica Scripta* **38**, 301 (1988).
 - ⁴⁴ A. Hartstein and Z. A. Weinberg, *J. Phys. C: Solid St. Phys.* **11**, L469 (1978).
 - ⁴⁵ C. C. Grimes, T. R. Brown, M. L. Burns, and C. L. Zipfel, *Phys. Rev. B* **13**, 140 (1976).

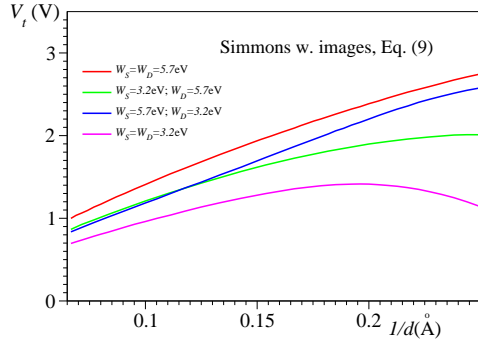
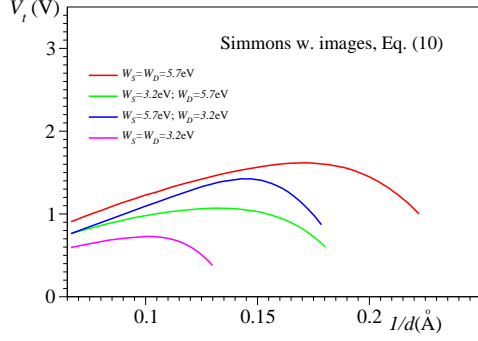
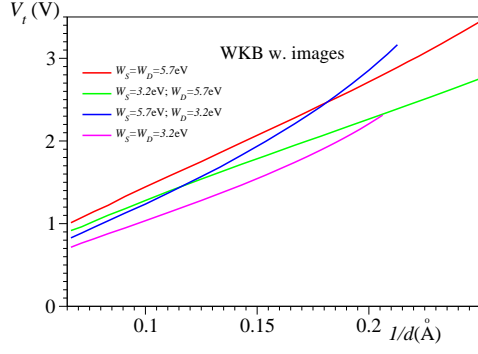
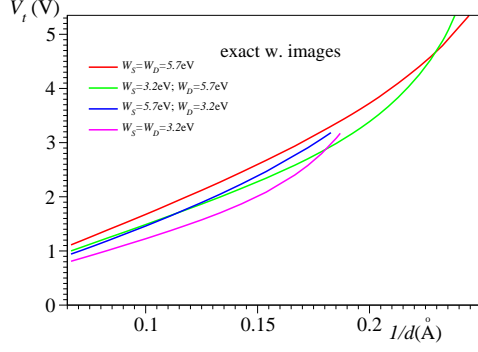


FIG. 5: Transition voltage for vacuum tunneling considering image effects computed exactly, and within the WKB and Simmons methods for electrodes with equal and different work functions $W_{S,D}$ specified in the legend. Simmons curves computed both with the incorrect [Eq. (10), panel c] and with the correct [Eq. (9), panel d] image forces are shown. Notice that, with our choice, the source/drain (S/D) is the negative/positive electrode and V_t -values are always positive.

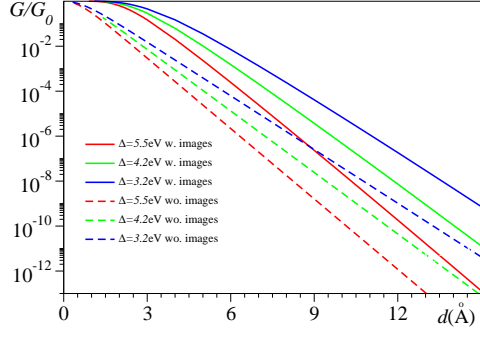


FIG. 6: Normalized conductance G/G_0 ($G_0 \equiv 2e^2/h$) computed with and without image effects versus nanogap width d for several apparent barrier heights Δ given in the legend. Without images $\Delta = W$, while with images $\Delta \simeq W - 0.57$ eV.